Cumhuriyet Sci. J., 44(2) (2023) 370-376
DOI: https://doi.org/10.17776/csj.1247286

Cumhuriyet Science Journal

| csj.cumhuriyet.edu.tr | Founded: 2002 ISSN: 2587-2680 e-ISSN: 2587-246X Publisher: Sivas Cumhuriyet University

The Energy Spectra of Electric Induced Mathieu Quantum Dot with Hydrogenic Impurity Implanted in Quantum Plasma

Mustafa Kemal Bahar [1,a,*]

[1] *Department of Physics, Faculty of Sciences, Sivas Cumhuriyet University, Sivas, Türkiye.*

**Corresponding author*

Research Article

History
Received: 03/02/2023
Accepted:04/04/2023

ABSTRACT

In this study, the energy spectra of the electric induced Mathieu quantum dot (MQD), containing the central hydrogenic impurity, fabricated by heterostructure $In_xGaAs_{1-x}/GaAs$, implanted in quantum plasma is considered. The effects of the external electric field, structural parameters and plasma screening on the energy levels of the MQD with the hydrogenic impurity are probed. The more general exponential cosine screened Coulomb (MGECSC) potential is used to depict the quantum plasma interactions. In order to solve the related Schrödinger equation, the numerical asymptotic iteration method (AIM) is employed. Achievable values of the effective potential parameters are taken into consideration, and for special purposes, the alternative to each other of these parameters is also evaluated.

Keywords: Quantum dot, Quantum plasma, Mathieu potential, Electric field, Electronic properties.

[a] *mussiv58@gmail.com* *https://orcid.org/0000-0003-4265-1402*

Introduction

Quantum dots are, in general, electron-confined systems. In these structures it is possible to confine one, two or more electrons. Quantum dots can be fabricated using various semiconductor materials. Quantum dots formed by $In_xGaAs_{1-x}/GaAs$ heterostructure will be considered in the present work, due to experimental advantages such as non-deformation of the growth material and sharp interface formation arising from reduced mixing in the formation of quantum dots [1]. The electronic and optical properties exhibited by the quantum dot are closely related to the confinement effects. A quantum dot is called as three-dimensional if the confinement effects of electrons are isotropic, but two-dimensional if one direction is more dominant than the other two in the encompassment effect [2]. Tuning the radiation frequencies of the quantum dot is possible by changing the size, shape, content and confinement effects of the quantum dot. The reason why quantum dots have technological reflections in a very important and wide area is the possibility of this frequency tuning. There are many experimental methods used in the production of quantum dots. Thanks to advanced nanofabrication methods, it is possible to synthesize quantum dots with different numbers of electrons and different surrounding geometries [3]. These types of quantum dots have been studied in detail both theoretically and experimentally [4-5]. Some experimental studies suggest that the optimal quantum dot profiles to encompass electrons should be of the well-like type [6]. Due to this experimental prediction, the Mathieu quantum dot (MQD), which exhibits a well-likeconfinement, will be considered in the present work [7-9]. Plasmas are a very important experimental argument for the experimental generation and modification of quantum dots [10,11]. Plasma environments can create a tuning mechanism on the electronic properties of quantum dots, thanks to the shielding effects caused by the complex correlation between the charged particles in them. The more general exponential cosine screened Coulomb (MGECSC) potential is predicted in a more detailed, more functional and more physical studying plasma interactions theoretically, and is expressed as [12-15]

$$V_{MGECSC}(r) = \frac{-Ze^2}{4\pi\varepsilon_0 r}(1+br)\exp\left(-\frac{r}{\lambda}\right)\cos\left(\frac{ar}{\lambda}\right), \qquad (1)$$

where a, b and λ are the plasma screening parameters. The MGECSC potential is more functional as it can be reduced to SC, ECSC and pure Coulomb (PC) potentials thanks to the parameters in its [15]. In this study, the effects of external electric field, structural factors and plasma shielding on the energy levels of the MQD with hydrogenic impurity, implanted in a quantum plasma environment modeled by the MGECSC potential are investigated. The motivation of the study is to compare the efficiency of the plasma shielding effect with the structural factors and the efficiency of the external electric field on energy levels. In this manner, it is important to do alternative parameter analysis.

The work is planned as follows: In the Section 2, the theoretical model and computation method are furnished. In Section 3, the finding are discussed. The last paragraph is allocated to the conclusions.

Theoretical Model and Computation Method

In order to obtain the energy spectra of the electric field induced MQD including the hydrogenic impurity at its centre, embedded in quantum plasma medium, the Hamiltonian operator whose eigenvalues must be found is given by

$$H = -\frac{\hbar^2\nabla^2}{2m^*} + V_{MQD}(r) + V_i(r) + V_{ef}(r), \quad (2)$$

where, $V_{MQD}(r)$ is the quantum dot confinement potential, $V_i(r)$ is the shielded impurity potential energy, $V_{ef}(r)$ is the potential energy term arising from the external electric field. They are given by

$$V_{MQD}(r) = V_0(sin^2(\eta r) - \cos(\eta r)), \quad (3)$$

$$V_i(r) = -\frac{Ze^2}{4\pi\varepsilon r}\exp(-r/\lambda)(1+br)\cos(ar/\lambda), \quad (4)$$

$$V_{ef}(r) = e\vec{\xi}.\vec{r}, \quad (5)$$

where, V_0 is the MQD depth parameter; η is the MQD width parameter; ε is the static dielectric constant in the material; a, b, and λ are the plasma screening parameters; ξ is the external electric field. Here it is assumed that $\vec{\xi}.\vec{r} = \xi r$. In this case, the wave equation to be solved to obtain the energy spectra is stated as

$$H\psi(r,\theta,\phi) = E\psi(r,\theta,\phi). \quad (6)$$

where, as the interaction system is the spherical symmetric, the angular solution is the spherical harmonics. In order to be able to find the eigenvalues of Eq.(6), the numerical asymptotic iteration method (AIM) is employed.

The AIM is a method that can provide both a numerical and, if possible, analytical solution. Here, the outline of AIM is outlined. For detail, please refer Refs.[16-18]. The AIM is a very functional and practical method to solve the following second-order differential equations.

$$y'' = \lambda_0(x)y' + s_0(x)y, \quad (7)$$

where, $\lambda_0(x) \neq 0$, ve $\lambda_0(r), s_0(r)$ are in $C_\infty(a,b)$. Also, $\lambda_0(x), s_0(x)$ are differentiable functions. The general physical solution of Eq.(7) is as follows

$$y(x) = \exp(-\int^x \upsilon dx'), \quad (8)$$

in that, for enough large n,

$$\frac{s_n(x)}{\lambda_n(x)} = \frac{s_{n-1}(x)}{\lambda_{n-1}(x)} \equiv \upsilon, \quad (9)$$

where

$$\lambda_n(x) = \lambda'_{n-1}(x) + s_{n-1}(x) + \lambda_0(x)\lambda_{n-1}(x),$$

$$s_n(x) = s'_{n-1}(x) + s_0(x)\lambda_{n-1}(x), n = 1,2,3 \ldots \quad 10)$$

The termination condition of the AIM is considered to obtain the energy spectra. This termination condition is expressed as

$$\Delta(x) = \lambda_{n-1}(x)s_n(x) - \lambda_n(x)s_{n-1}(x) = 0. \quad (11)$$

The quantum dot radius is taken as $R_{dot} = 6a_0$ throughout the study as well as $m^* = 0.067m_0$, $\varepsilon_{GaAs} = 13.18$. The effective Bohr radius are calculated as $a_0 = 103.7A^o$, respectively.

Results and Discussion

In this study, the energy spectrum of an external electric field induced MQD with central hydrogenic impurity implanted in a quantum plasma is investigated. In the study, the effect of 6 parameters, namely plasma shielding parameters (a, b ve λ), external electric field strength parameter (ξ), and structural parameters ((x, *In*-concentration and η, quantum dot width) are taken into account. The relevant range of these parameters is within the experimentally achievable limit. The effective potential profile, which includes the MQD potential for the effect of each parameter, is also examined. Here it should be pointed out that although certain quantum levels are considered for the spectrum of the MQD, it is also possible to calculate for arbitrary quantum levels. In addition, since the motivation of the study is based only on the energy spectrum, the wave functions are not examined.

In Figure 1a, when $\xi = 10$kV/cm, the energy values for some quantum levels of the MQD with $\eta = 0.25a_0^{-1}$ implanted in the quantum plasma presented by the MGECSC potential with $a = 1, b = 1a_0^{-1}$ and $\lambda = 10a_0$ are demonstrated as a function of In-concentration x. In Figure 1b, the effective potential profile with $\ell = 1$ for different In-concentrations is displayed in synchronization with the parameter set in Figure 1a.

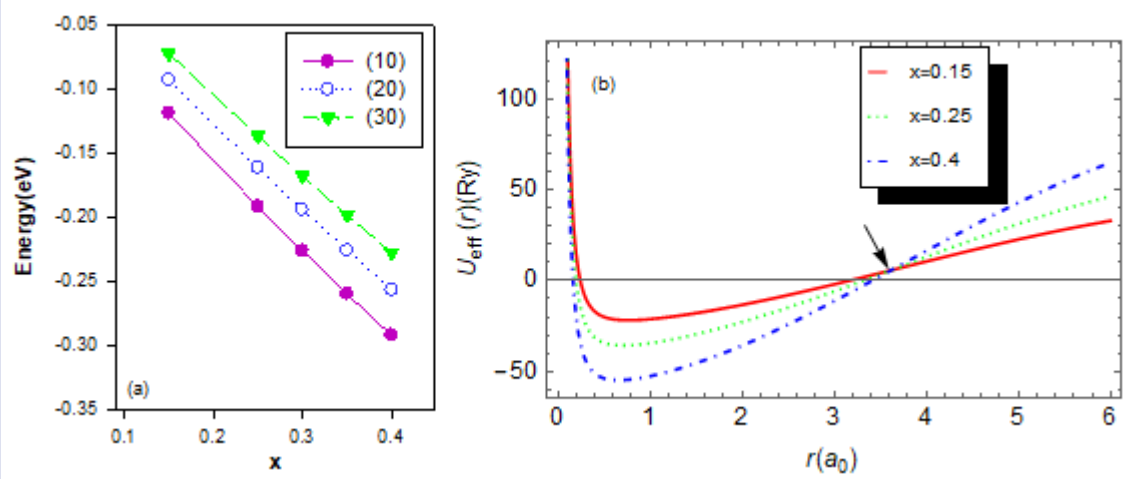

Figure 1. When $\xi = 10$kV/cm, the energy values for some quantum levels of the MQD with $\eta = 0.25a_0^{-1}$ implanted in the quantum plasma presented by the MGECSC potential including with $a = 1, b = 1a_0^{-1}$ and $\lambda = 10a_0$, as a function of x, b) the effective potential profile with $\ell = 1$ in synchronization with the parameter set in panel (a).

Figure 1a shows the energy of the first three quantum levels for only $\ell = 0$. As seen, as the *In*-concentration increases, the energies of the quantum levels decrease significantly. In Figure 1b, it is clear that the increment of *In*-concentration increases the potential strength and makes it more attractive. The bound state localizations in a more attractive potential are lowered (See Figure 1a). Here another remarkable one is that after approximately $R_{dot} \cong 3.8a_0$ of the MQD spatial limitation, the augment of *In*-concentration causes the effective potential profile having an inverse character compared to before one. However, it seems that the effective potential exhibits the character before this critical threshold. Because increasing x decreases the bound state energies. Since the energy difference between the bound state localizations will increase in a deepening potential profile, it is expected that the resonant frequencies of some nonlinear optical properties shift to blue.

In Figure 2a, when $\xi = 10$kV/cm, the energy values for some quantum levels of the MQD with $x = 0.4$ implanted in the quantum plasma presented by the MGECSC potential potential including with $a = 1, b = 1a_0^{-1}$ and $\lambda = 10a_0$, are presented as a function of MQD width parameter η.

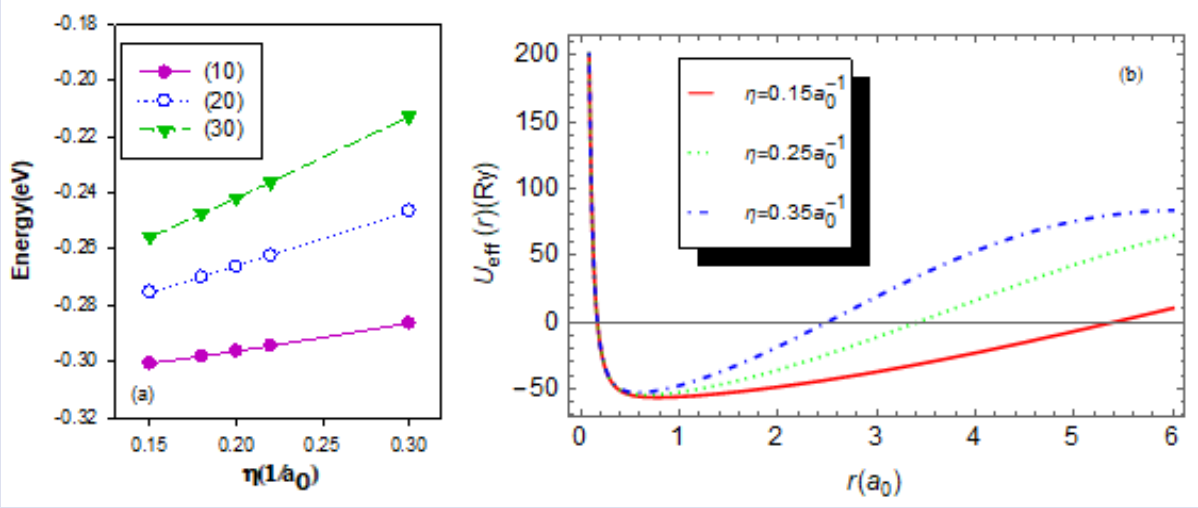

Figure 2. a) When $\xi = 10$kV/cm, the energy values for some quantum levels of the MQD with $x = 0.4$ implanted in the quantum plasma presented by the MGECSC potential potential including with $a = 1, b = 1a_0^{-1}$ and $\lambda = 10a_0$, as a function of η, b) the effective potential profile with $\ell = 1$ in synchronization with the parameter set in panel (a).

As seen in Figure 2a, increasing the MQD width parameter enhances the bound state energy values. Because the increase of the parameter η increases the repulsion of the effective potential (See Figure 2b). In the potential profile with increased repulsion, the bound state localizations increase. Also, the energy difference between the bound state localizations increases. This increase is also confirmed in Figure 2a. When considering Figure 2a, it is observed that there is an augment between the energy levels as the parameter η increases. Due to this augment, it may be said that the resonant frequencies of the nonlinear optical properties of the MQD exhibit the blue-shifting.

In Figure 3a, the energy values for some quantum levels of of the MQD with $x = 0.4, \eta = 0.25a_0^{-1}$ implanted in the quantum plasma presented by the MGECSC potential potential including with $a = 1, b = 1a_0^{-1}$ and $\lambda = 10a_0$, are represented as a function of the external electric field parameter ξ.

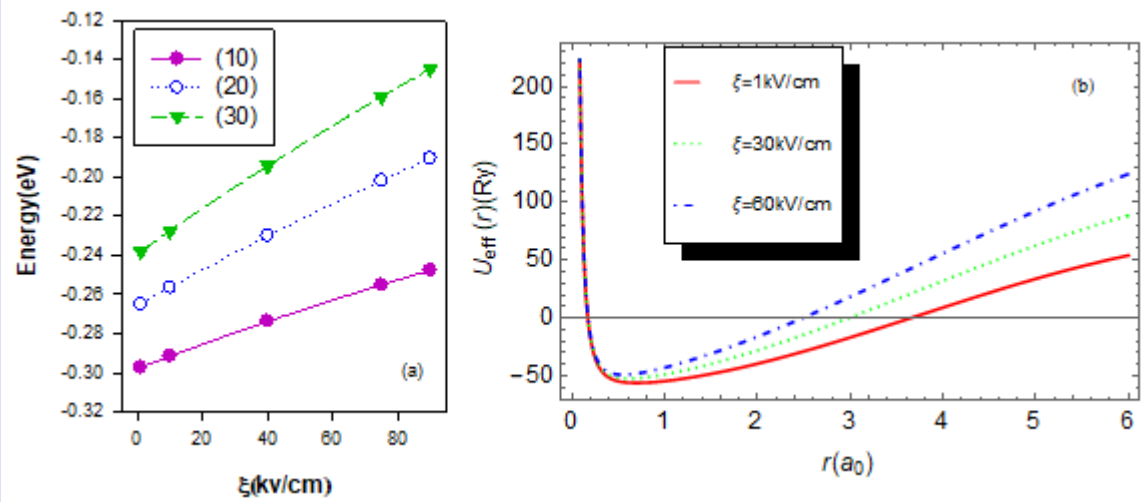

Figure 3. a)The energy values for some quantum levels of of the MQD with $x = 0.4, \eta = 0.25a_0^{-1}$ implanted in the quantum plasma presented by the MGECSC potential potential including with $a = 1, b = 1a_0^{-1}$ and $\lambda = 10a_0$, as a function of ξ, b) the effective potential profile with $\ell = 1$ in synchronization with the parameter set in panel (a).

As seen in Figure 3a, the increment in the external electric field strength increases the energy values of the respective quantum levels. Because the increase in the external electric field strength increases the repulsion of the effective potential (See Figure 3b). In this case, new localizations are expected to rise, which is confirmed in Figure 3a. In addition to the enhancement of the bound state localizations formed in the profile in Figure 3b, the energy differences between them are expected to increase.

As seen in Figure 3a, the increase in the external electric field strength increases the difference between the respective quantum levels. It can be said that this increase in difference may cause the nonlinear optical properties of MQD to shift the resonant frequencies to blue.

In Figure 4a, when $\xi = 10$kV/cm, the effective potential profile of the MQD with $x = 0.4, \eta = 0.25a_0^{-1}$ implanted in the quantum plasma presented by the MGECSC potential potential are plotted, in panel (a), when $a = 1, b = 1a_0^{-1}$, for different λ parameter values as a function of the radial direction (r); in panel (b), when $a = 1, \lambda = 10a_0$, for different b parameter values as a function of the radial direction (r); in panel (c), when$b = 1a_0^{-1}, \lambda = 10a_0$, for different a parameter values as a function of the radial direction (r). Here it is important to note that the potential profiles in Figure 4 are synchronized with Tables 1,2 and 3, respectively, in terms of parameter sets.

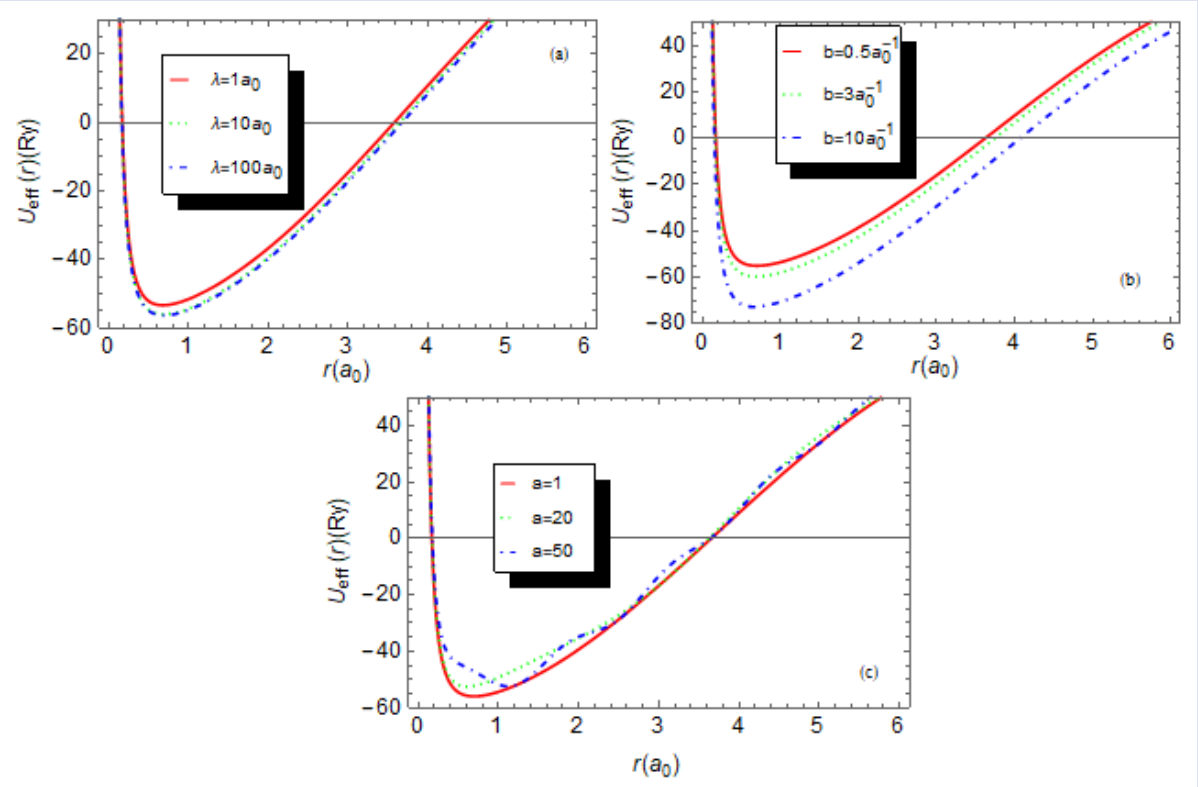

Figure 4. When $\xi = 10$kV/cm, the effective potential profile of the MQD with $x = 0.4, \eta = 0.25a_0^{-1}$ implanted in the quantum plasma presented by the MGECSC potential potential are plotted, in panel (a), when $a = 1, b = 1a_0^{-1}$, for different λ parameter values as a function of the radial direction (r); in panel (b), when $a = 1, \lambda = 10a_0$, for different b parameter values as a function of the radial direction (r); in panel (c), when$b = 1a_0^{-1}, \lambda = 10a_0$, for different a parameter values as a function of the radial direction (r).

In Table 1, when $\xi = 10$kV/cm, the energy values for some quantum levels of the MQD with $x = 0.4$ implanted in the quantum plasma presented by the MGECSC potential potential including with $a = 1, b = 1a_0^{-1}$ and $\lambda = 1 - 10 - 100 - 500a_0$, are furnished in eV unit. As seen in Table 1, the increment of λ parameter leads to decrease the energy values of the bound state. However, this decrease becomes monotonous at large values of λ. Therefore, small regimes are more suitable for the functional range of λ, which is an expected situation. Because at sufficiently large values of λ, the interaction potential exhibits Coulombic character, and the plasma shielding is less felt. Decrease in the bound state localizations (See Table 1) weakly increases the attractiveness of the effective potential due to the increase in λ (See Figure 4a).This causes their energy level to lift down faintly. Besides, it is clear that the parameter λ does not have a significant effect on the differences between energy levels. Therefore, it can be said that the parameter λ is not functional on the resonant frequencies of some nonlinear optical properties, except for the tuning that can be made with small λ regimes in systems with sensitive frequency requirements.

Table 1: When $\xi = 10$kV/cm, the energy values for some quantum levels of the MQD with $x = 0.4, \eta = 0.25a_0^{-1}$ implanted in the quantum plasma presented by the MGECSC potential potential including with $a = 1, b = 1a_0^{-1}$ and $\lambda = 1 - 10 - 100 - 500a_0$, in eV unit.

$(n\ell)$	$\lambda = 1a_0$	$\lambda = 10a_0$	$\lambda = 100a_0$	$\lambda = 500a_0$
(10)	-0.278211106611	-0.291501806989	-0.293013116151	-0.293147807383
(20)	-0.220340993620	-0.234318701486	-0.236232079492	-0.23640317908
(30)	-0.168186518338	-0.181910613646	-0.184107444614	-0.184304583361
(11)	-0.242266526524	-0.256477349404	-0.258262933377	-0.258422345642
(21)	-0.189873771657	-0.203922691933	-0.206012117004	-0.206199293668
(31)	-0.139976576236	-0.153569499145	-0.155906031947	-0.156116096074
(12)	-0.212884712082	-0.291501806989	-0.256477349404	-0.227395230788
(22)	-0.162537463664	-0.234318701486	-0.203922691933	-0.176565875165
(32)	-0.113925943360	-0.181910613646	-0.153569499145	-0.127389894947

In Table 2, when $\xi = 10$kV/cm, the energy values for some quantum levels of the MQD with $x = 0.4$ implanted in the quantum plasma presented by the MGECSC potential potential including with $a = 1, b = 0.5 - 2.5 - 5 - 10a_0^{-1}$ and $\lambda = 10a_0$, are furnished in eV unit. An increase in the b plasma parameter causes a linear decrease in the bound state energy values (See Table 2). The reason for this decrease is that the effective potential becomes more attractive due to the increase of the b parameter, as can be seen in Figure 4b. As can be seen, the increase of the b parameter has a significant function on the optical properties of the system. However, the difference between the energy levels is almost unchanged, as the increase of the b parameter creates a perfectly symmetrical attraction in the effective potential profile. From here, the following can be concluded that the b parameter is ineffective on the resonant frequencies of some nonlinear optical properties of the MQD.

Table 2: When $\xi = 10$kV/cm, the energy values for some quantum levels of the MQD with $x = 0.4, \eta = 0.25a_0^{-1}$ implanted in the quantum plasma presented by the MGECSC potential potential including with $a = 1, b = 0.5 - 2.5 - 5 - 10a_0^{-1}$ and $\lambda = 10a_0$, in eV unit.

$(n\ell)$	$b = 0.5a_0^{-1}$	$b = 2.5a_0^{-1}$	$b = 5a_0^{-1}$	$b = 10a_0^{-1}$
(10)	-0.286578039947	-0.306277296948	-0.330916740495	-0.380244358712
(20)	-0.229620036540	-0.248419869438	-0.271938800332	-0.319038468753
(30)	-0.177371320523	-0.195534105491	-0.218258396788	-0.263774521260
(11)	-0.251706812079	-0.270794451246	-0.294674227602	-0.342498483771
(21)	-0.199322802181	-0.217728063413	-0.240755746965	-0.286879354594
(31)	-0.149108855877	-0.166957413886	-0.189290303123	-0.234028118382
(12)	-0.222737268674	-0.241375143811	-0.264694745172	-0.311405530092
(22)	-0.172052900062	-0.190110922134	-0.212706120618	-0.257969901577
(32)	-0.123002784625	-0.140557572469	-0.162524590908	-0.206535031193

In Table 3, when $\xi = 10$kV/cm, the energy values for some quantum levels of the MQD with $x = 0.4$ implanted in the quantum plasma presented by the MGECSC potential potential including with $a = 1 - 5 - 10 - 30, b = 1a_0^{-1}$ and $\lambda = 10a_0$, are furnished in eV unit. The increase of the a plasma parameter causes an increase in the bound state energy values (See Table 3). The increment here has a certainty at larger values of a, due to the oscillation in the plasma potential arising from the cosine term. As the a plasma parameter increases, the stable structure of the effective potential deteriorates and a more aggressive repulsion occurs in the potential (See Figure 4c). In strong regimes of a, besides the increase in bound state levels caused by this repulsion, the energy difference between some levels decreases. In this case, it can be stated that the red-shifting can realize in the resonant frequencies of some nonlinear optical features of the MQD.

Table 3: When $\xi = 10$kV/cm, the energy values for some quantum levels of the MQD with $x = 0.4, \eta = 0.25a_0^{-1}$ implanted in the quantum plasma presented by the MGECSC potential potential including with $a = 1 - 5 - 10 - 30, b = 1a_0^{-1}$ and $\lambda = 10a_0$, in eV unit.

$(n\ell)$	$a = 1$	$a = 5$	$a=10$	$a = 30$
(10)	-0.291501806989	-0.290309932655	-0.286869363563	-0.264162803777
(20)	-0.234318701486	-0.231852530744	-0.225335545505	-0.210165328050
(30)	-0.181910613646	-0.178407132431	-0.170052579468	-0.166759219919
(11)	-0.256477349404	-0.254506904882	-0.249034187397	-0.224308352546
(21)	-0.203922691933	-0.200858425688	-0.193146676584	-0.184757937524
(31)	-0.153569499145	-0.149556480957	-0.140511711773	-0.139052137697
(12)	-0.227395230788	-0.224780394058	-0.217772080671	-0.198693456784
(22)	-0.176565875165	-0.172958960142	-0.164278012201	-0.159028236265
(32)	-0.127389894947	-0.122900343357	-0.113300885223	-0.112274549821

The results of this study can be summarized as follows: Some energy levels of electric field induced MQD with hydrogenic impurity, implanted in quantum plasma modeled by the MGECSC potential have been investigated. Structural parameters are functional and dominant over the electronic properties of the system. However, although the external electric field strength is an external factor, it is effective on energy levels. In this context, since both ξ and η parameters increase the energy levels, the ξ and η parameters may be alternative to each other. The effect of plasma shielding is quite feeble compared to structural factors and external electric

field effect. While the λ parameter, which can be considered as the most important plasma screening parameter, is effective in small regimes, it is not effective in strong regimes. Although the b parameter lowers the energy levels, it is not effective on the energy difference between the levels due to its linear effect. This means that the b parameter will not have observable effect on the resonant frequency of some nonlinear optical properties. At large values of the a plasma parameter, some levels converge due to the aggressive repulsion. To summarize, for the relevant system, the structural and external electric field effects are functional, whereas plasma shielding effects are not. For the relevant system, plasma shielding is effective on electronic properties but not on possible optical properties. Because plasma shielding has a very feeble effect on the difference between energy levels.

Conflicts of interest

There are no conflicts of interest in this work.

References

[1] Liculescu E. C., Bejan D., Nonlinear optical properties of GaAs pyramidal quantum dots: Effects of elliptically polarized radiation, impurity, and magnetic applied fields, *Physica E: Low-dimensional Systems and Nanostructures*, 74 (2015) 51-58.

[2] Harrison P., *Quantum Wells, Wires, Dots* (2. Edition). England:Wiley, (2005).

[3] Jacak L., Semiconductor quantum dots-towards a new generation of semiconductor devices, *European Physical Journal*, 21 (2000) 487-497.

[4] Xie W. F., Two interacting electrons in a Gaussian confining potential quantum dot, *Solid State Communications*, 127 (2003) 401-405.

[5] Owen J., Brus L. Chemical synthesis and luminescence applications of colloidal semiconductor quantum dots, *Journal of American Chemical Society*, 139 (2017) 10939-10943.

[6] Davies J. H., *The Physics of Low-Dimensional Semiconductors: An Introduction* (5.Edition). USA:Cambridge, (1999).

[7] Başer P, Bahar M. K., Evaluation of the external electric- and magnetic field-driven Mathieu quantum dot's optical observables, *Physica B:Condense Matter*, 639 (2022) 413991-413999.

[8] Bahar M. K, Başer P., Nonlinear optical characteristics of thermodynamic effects-and electric field-triggered Mathieu quantum dot, *Micro and Nanostructures*, 170 (2022) 207371-207382.

[9] Bahar M. K, Başer P., Tuning of nonlinear optical characteristics of Mathieu quantum dot by laser and electric field, *The European Physical Journal Plus*, 137 (2022) 1138-1148.

[10] Kortshagen U., Nonthermal plasma synthesis of semiconductor nanocrystals, *Journal of Physics D: Applied Physics*, 42 (2009) 113001-113023.

[11] Pi, X. D., Kortshagen, U., Nonthermal plasma synthesized freestanding silicon–germanium alloy nanocrystals, *Nanotechnology*, 20 (2009) 295602-295608.

[12] Bahar M. K., Soylu A., Two-electron quantum dot in plasmas under the external fields, *Physics of Plasmas*, 25 (2018) 022106-022118.

[13] Bahar M. K., Soylu A., Confinement control mechanism for two-electron Hulthen quantum dots in plasmas, *Journal of Physics B:Atomic, Molecular and Optical Physics*, 51 (2018) 105701-105715.

[14] Bahar M. K., Soylu A., Laser-driven two-electron quantum dot in plasmas, *Physics of Plasmas*, 25 (2018) 062113-062125.

[15] Bahar M. K., Plasma screening effects on the energies of hydrogen atom under the influence of velocity-dependent potential, *Physics of Plasmas*, 21 (2014) 072706-072716.

[16] Ciftci H., Hal R. L., Saad N., Asymptotic iteration method for eigenvalue problems, *Journal of Physics A: Mathematical and General*, 36 (2003) 11807-11816.

[17] Ciftci H., Hall R. L., Saad N., Construction of exact solutions to eigenvalue problems by the asymptotic iteration method, *Journal of Physics A: Mathematical and General*, 38 (2005) 1147-1155.

[18] Saad N., Ciftci H., Hall R. L., Criterion for polynomial solutions to a class of linear differential equations of second order, *Journal of Physics A: Mathematical and General*, 39 (2005) 13445-13454.